Bull Earthquake Eng (2011) 9:1617–1642
DOI 10.1007/s10518-011-9291-1

ORIGINAL RESEARCH PAPER

# The relevance of energy damping in unreinforced masonry rocking mechanisms. Experimental and analytic investigations

**Luigi Sorrentino · Omar AlShawa · Luis D. Decanini**

Received: 28 October 2010 / Accepted: 2 June 2011 / Published online: 19 June 2011


**Abstract** Existing unreinforced masonry buildings frequently suffer out-of-plane local collapse mechanisms when undergoing earthquake ground motion. The energy damping that occurs during the motion, due to impacts of a wall against the foundation or against other walls, is a relevant parameter on the response. An experimental investigation has been carried out to estimate the dissipation of kinetic energy that takes place during free oscillations. Restraint conditions allow for two-sided rocking (wall resting on a foundation) and one-sided rocking (wall resting on a foundation adjacent to transverse walls). Five specimens have been tested, modelling walls acted out-of-plane (façades). When one-sided rocking is under consideration, different depths of the contact surface between façade and transverse walls are considered. In the case of two-sided rocking, the experimental coefficient of restitution is slightly lower than the analytic coefficient. In the case of one-sided rocking, an analytic formulation is proposed and this is compared against experimental data. Although the coefficient of restitution of one-sided rocking is less than half that of two-sided rocking, it is not equal to zero. Thus, it cannot induce a sudden stop of the motion. Hence, nonlinear time history analyses performed under this assumption may prove unsafe. Moreover, a comparison has been carried out between overturning maps, induced by twenty natural accelerograms, computed for the analytic coefficient of restitution and those computed for the experimental coefficient of restitution. The increased energy dissipation reduces the frequency of overturning and causes a more regular behaviour.

**Keywords** Impulsive energy dissipation · Experimental coefficient of restitution · Analytic coefficient of restitution · Two-sided rocking · One-sided rocking

L. Sorrentino (✉) · O. AlShawa · L. D. Decanini
Dipartimento di Ingegneria Strutturale e Geotecnica, Università degli Studi di Roma "La Sapienza", via Antonio Gramsci 53, 00197 Rome, Italy
e-mail: luigi.sorrentino@uniroma1.it

## 1 Introduction

Existing unreinforced masonry buildings frequently suffer out-of-plane local collapse mechanisms when affected by strong earthquake ground motion (Decanini et al. 2000, 2004; D'Ayala and Speranza 2003). In recent years several authors have assessed the earthquake stability of such mechanisms through non linear time history analyses (Griffith et al. 2003; Lam et al. 2003; Liberatore and Spera 2003; Goretti et al. 2007; Lagomarsino and Resemini 2009). The advantages of dynamic analyses compared to static analyses are well known. The structural behaviour is modelled more accurately and the role of conventional assumptions is markedly reduced. However, in order to obtain meaningful results a careful representation of the non linear mechanical behaviour of the response and of energy dissipation is necessary.

Up until now, the investigation of the estimation of energy damping and of its relevance to the response has received little attention in scientific literature. In particular, experimental tests have been very limited. Nonetheless, previous studies have shown that energy damping can be crucial to the response (Yim et al. 1980; Sorrentino et al. 2008a).

From a theoretical point of view, the most common approach is that of the conservation of angular momentum, used in conjunction with the classical hypotheses of impulsive dynamics: infinitesimal duration of impact, no displacement during impact, instantaneous variation of velocity during impact (Housner 1963; Spanos et al. 2001; De Lorenzis et al. 2007; Sorrentino et al. 2008b). This approach makes the estimation of energy damping possible for any mechanism for which the geometrical parameters are known. For example, Housner (1963), in considering two-sided rocking (in the following abbreviated as $2s$), finds an analytic velocity reduction factor $e_{an,2s}$ (also referred to as the analytic coefficient of restitution), equal to:

$$e_{an,\,2s} = \frac{\dot{\theta}^{+}}{\dot{\theta}^{-}} = 1 - 2\frac{mR^2}{I_O}\sin^2\alpha \tag{1}$$

with θ = rotation of the wall, dot indicating derivative with respect to time, superscript + (−) value after (before) impact, $m$ = mass of the wall, $R$ = distance of the centre of mass from the rocking hinge (Fig. 1), $I_o$ = polar moment of inertia with respect to the rocking hinge, $\alpha$ = angle between the vertical line through the rocking hinge and the inclined line through the rocking hinge and the centre of mass (Fig. 1). If the wall is homogeneous the previous equation becomes:

$$e_{an,\,2s} = 1 - \frac{3}{2}\sin^2\alpha = \frac{2\varsigma^2 - 1}{2\left(\varsigma^2 + 1\right)} \tag{2}$$

with $\varsigma = h/b$, height-to-thickness ratio of the wall.

The larger the coefficient of restitution, the smaller the energy dissipation. According to this approach, both material properties and size of the body are irrelevant upon damping. The Housner model for energy dissipation has been proved accurate on average, albeit with some scatter, by tests on a marble block rocking on a marble foundation (Liberatore et al. 2002). Similar results have been obtained previously for a concrete block with an aluminium base rocking on a steel foundation (Aslam et al. 1980): the experimental coefficient of restitution was equal to 0.925, compared to an analytic one of 0.942. Conversely, experimental damping has been found to be smaller than expected in very stocky oscillators, rather far-off from the height-to-thickness ratios of unreinforced masonry walls (Priestley et al. 1978; Lipscombe and Pellegrino 1993).

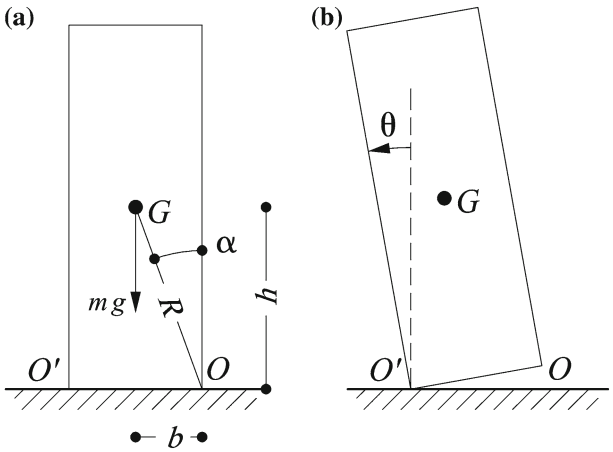


**Fig. 1** Parapet wall: geometrical parameters and displaced configuration. $g$ = gravity acceleration

Energy dissipation in rocking mechanisms has also been interpreted in terms of equivalent viscous damping, with values of approximately 3% in a parapet wall with $\varsigma = 8$ (Lam et al. 1995), and 5% in a vertical spanning strip wall with $\varsigma = 14$ (Griffith et al. 2004).

Granite blocks, with $\varsigma = 3 \div 8$, rocking on a granite foundation have also been tested in free oscillations (Peña et al. 2007). The experimental coefficient of restitution, $e_{exp}$, was found to converge to $e_{an,2s,}$ as $\varsigma$ increased.

No experimental program on unreinforced masonry wall energy damping seem to have been carried out so far. Previous tests (Lam et al. 1995; Griffith et al. 2004) have not been interpreted within a general theoretical framework, such as that of impulsive mechanics. Moreover, no tests whatsoever have been performed on one-sided rocking mechanisms. So far there is no mechanical model to assess energy dissipation for this kind of boundary condition, although it can be rather frequent in historical constructions. Therefore, previous investigators have assumed very small energy dissipation, usually equal to two-sided rocking (Hogan 1992), or very large energy dissipation, with no motion after impact (Liberatore and Spera 2003).

All the previous considerations suggest the advisability of an experimental program focused on energy dissipation in unreinforced masonry rocking mechanisms. The program will be presented in Sect. 2. In Sect. 3 a refined assessment of the coefficient of restitution, experimentally calibrated, will be presented. Moreover, an analytical formulation of the coefficient of restitution for one-sided rocking will be proposed. In Sect. 4 other parameters, measured during the tests, will be discussed. In Sect. 5 the influence of a refined estimation of energy dissipation on non linear time history analyses of rocking mechanisms will be examined. Finally, in Sect. 6 conclusions are presented.

## 2 Experimental tests

### 2.1 Test setup

The experimental campaign described here investigates rocking energy dissipation with the variation of: (1) boundary condition, (2) wall height-to-thickness ratio, (3) contact depth

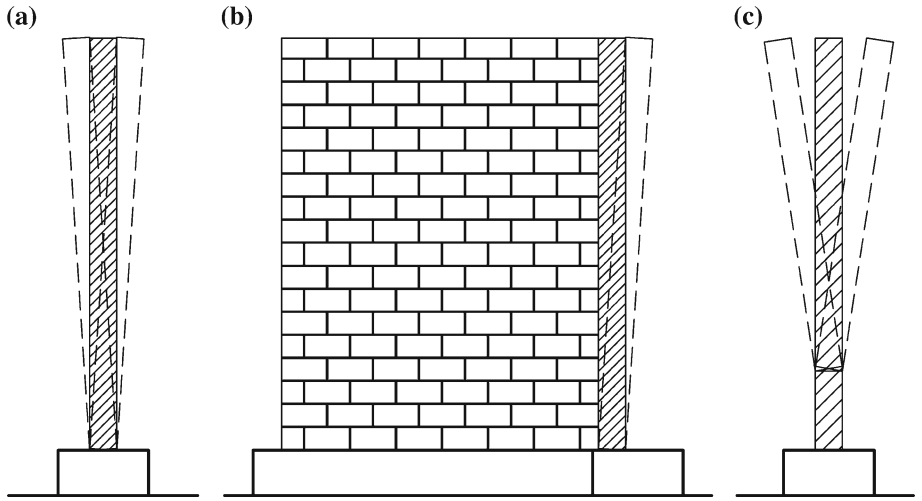


**Fig. 2** **a** Two-sided rocking, **b** one-sided rocking, **c** wall fractured above the base in order to get a different height-to-thickness ratio

between façade and transverse walls (one-sided rocking only), (4) unit material, (5) effect of test repetition.

Two boundary conditions are taken into account: (a) wall resting on a foundation (undergoing *two-sided* rocking, Fig. 2a); (b) wall resting on a foundation and adjacent to two transverse walls (undergoing *one-sided* rocking, Fig. 2b). The rocking walls are meant to model unreinforced masonry façades moved out-of-plane by earthquake-induced inertia forces. The condition of a two-sided rocking wall is typical of parapet, boundary, or archaeological walls (Fig. 3a). The condition of a one-sided rocking wall is peculiar to façades built without an efficient interlocking with transverse walls, due either to poor construction, or to building readjustments or to inadequately repaired damage from a previous earthquake (Tobriner et al. 1997, Fig. 3b).

The walls tested have characteristics which are common in Mediterranean existing buildings in terms of aspect ratios (height/thickness and length/thickness ratios) and materials, but the size is reduced to meet cost and facility limitations (Table 1). The height-to-thickness ratio was varied because it is the governing parameter of energy dissipation, according to the impulsive mechanics approach of Eq. (2). In order to increase the number of tests and because of the very limited damage accumulation observed, the walls were fractured at an intermediate bed joint, thus obtaining a shorter specimen (Fig. 2c). Height/thickness ratio varies between 6.5 and 14.6 (Table 2). In one-sided rocking tests, the ratio between contact depth and wall length was also varied (Fig. 4). This makes it possible to simulate different transverse-wall densities and their influence on energy dissipation.

The specimens are solid, single-wythe. The program provides for five walls to be rocked (façades), and two walls to be used as transverse walls in one-sided rocking tests. Transverse walls and two of the façades are built using tuff units, quarried in Riano (Central Italy); the units are 370 mm long, 123 mm wide, 110 mm thick. The remaining three façades are manufactured with solid clay bricks, 235 mm long, 113 mm wide, 53 mm thick. This makes it possible to assess the influence of the unit material on energy dissipation. The mortar is always pozzuolanic (1:0.1:3, lime:cement:pozzuolan), laid in 10 mm joints in brick masonry and in 20 mm joints in tuff masonry. Units were wetted before laying. The faces of the

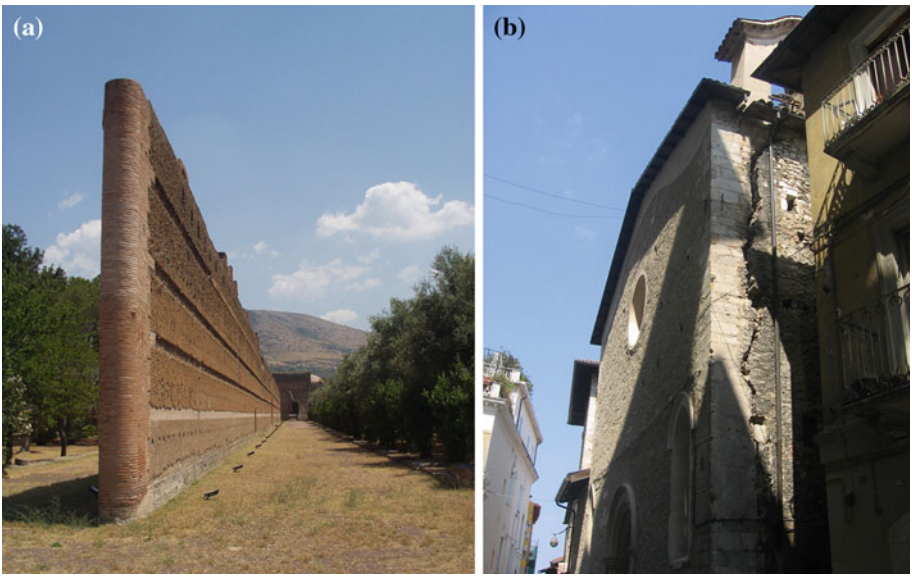


**Fig. 3** **a** Wall prone to two-sided rocking: Pecile in Villa Adriana, Tivoli (close to Rome, Italy); **b** Wall after one-sided rocking: Oratory of San Giuseppe dei Minimi, L'Aquila (Central Italy), after the April 6, 2009 earthquake

**Table 1** Walls' main features

| Wall | Size (length × height × thickness) (mm × mm × mm) | Unit |
|---|---|---|
| 1 | 1420 × 1090 × 113 | Solid clay brick |
| 2 | 1440 × 1630 × 113 | Solid clay brick |
| 3 | 1500 × 1780 × 123 | Tuff |
| 4 | 1030 × 1630 × 113 | Solid clay brick |
| 5 | 1130 × 1800 × 123 | Tuff |
| 6–7[a] | 1490 × 1820 × 260 | Tuff |

[a] used as transverse walls in one-sided rocking tests

transverse walls adjacent to the façades were plastered, in order to reduce the roughness of the contact surface. All the walls are built on a masonry foundation laid in a steel case. The fracture induced in the rocking hinge always occurred at the interface between unit and mortar.

The behaviour of the walls due to the imposed displacement is a rigid body one. Therefore, material mechanical properties do not have a great effect. However, some tests were performed in order to obtain a more complete description of the specimens. More extensive details are presented elsewhere (Sorrentino et al. 2008c; Decanini et al. 2009), here only mean values are reported.

The brick's mean bulk specific weight is 18.1 kN/m$^3$, while mean compressive strength is 45.5 MPa. This value, although reasonable, might be an overestimation, because the test was performed on the entire unit (Binda et al. 1996).

The tuff's mean bulk specific weight is 12.8 kN/m$^3$, while mean compressive strength is 5.9 MPa. The first value is lower and the second value higher than reported in the literature (Augenti and Parisi 2009). However, Latium tuff frequently presents such features.

**Table 2** Height of specimens obtained from walls of Table 1, by means of fracturing at an intermediate bed joint

| Specimen | Height (mm) | Height/Thickness | Number of valid tests performed: two-sided | Number of valid tests performed: one-sided | | |
|---|---|---|---|---|---|---|
| | | | | CD= 260 (mm) | CD= 120 (mm) | CD= 60 (mm) |
| 1a | 1090 | 9.6 | 10 | 0 | 0 | 0 |
| 1b | 800 | 7.1 | 9 | 9 | 10 | 0 |
| 1c | 820 | 7.3 | 0 | 16 | 21 | 17 |
| 2a | 1630 | 14.4 | 15 | 29 | 16 | 29 |
| 2b | 1360 | 12.0 | 19 | 13 | 14 | 14 |
| 3a | 1630 | 13.3 | 5 | 29 | 26 | 18 |
| 3b | 1280 | 10.4 | 8 | 17 | 20 | 0 |
| 4a | 1560 | 13.8 | 0 | – | – | – |
| 4b | 1170 | 10.4 | 19 | – | – | – |
| 5a | 1790 | 14.6 | 28 | – | – | – |
| 5b | 1190 | 9.7 | 20 | – | – | – |
| 5c | 800 | 6.5 | 21 | – | – | – |

The mortar's mean bulk specific weight is 17.5 kN/m$^3$. Its mean compressive strength is 7.4 MPa. Mean tensile strength, measured through the cylinder splitting test, is 1.25 MPa. Such figures are comparable with those reported in the literature (Bernardini et al. 1984), but are nonetheless rather high. They help to explain the limited damage accumulation and the monolithic behaviour observed.

Test repetition was examined in terms of variation of energy dissipation and variation of displacement capacity. Both proved to be limited. Therefore walls 1-3, which were initially only to be tested in one-sided rocking, were also tested in two-sided rocking. The total number of tests performed is 614. However, only 452 were considered valid, due to instrument malfunction, disturbed initial conditions and so on. Moreover, tests with a residual top out-of-plumb larger than 1.5 mm were also excluded. The 1.5 mm limit was chosen as a tolerance comparable to the one for the perfectly vertical and adjacent positioning of façade and transverse walls.

During each test only displacements are measured, because the accelerations feel the effect of the sudden reduction of velocity upon impact. Six inductive displacement transducers are used (Fig. 5) in order to evaluate the activation of degrees of freedom other than the expected out-of-plane rotation, as explained in the following paragraph. Channel 5 was only used in one-sided rocking tests, in order to evaluate possible deformation upon impact against transverse walls. The instruments were fixed on external frames. Preliminary tests ruled out any disturbance of the frames due to the rocking of the wall. Sampling frequency, initially set at 100 Hz, was increased to 400 Hz, the value used by previous investigators (Liberatore and Spera 2001b).

Several possibilities were considered in order to release the displaced wall. Initial solutions (the burning of a rope or hand release) were rejected because they led to a disturbance of initial conditions. Eventually, due to the monolithic behaviour observed, the wall was laid against a safety structure, with rotation $\theta$ slightly larger than the instability rotation ($\theta = \alpha$). Then, the wall was very slowly pushed by means of a screw device. Figure 6 illustrates a

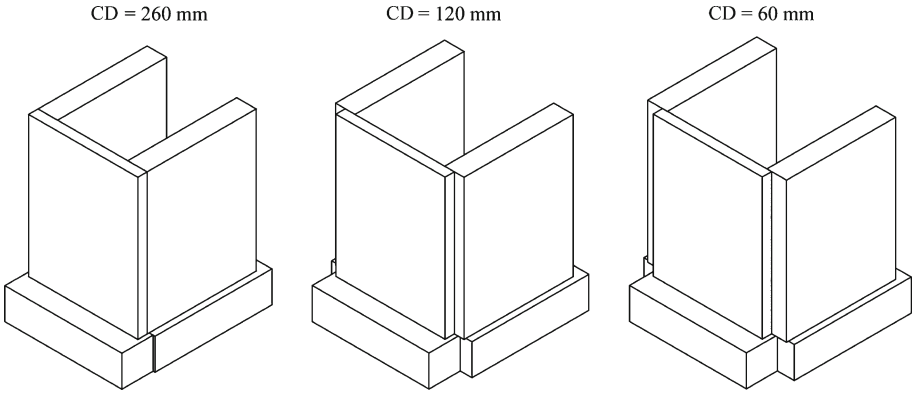


**Fig. 4** One-sided rocking: contact depth, CD, between façade and transverse walls

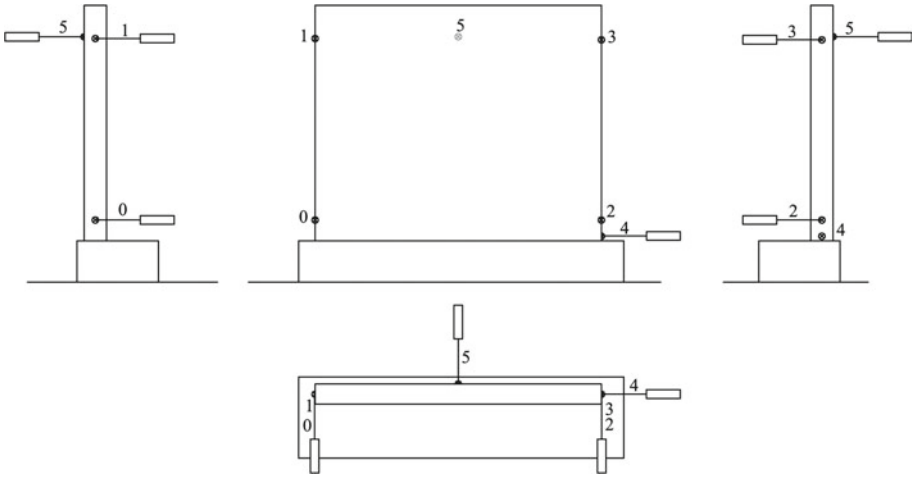


**Fig. 5** Experimental setup. Position of the six transducers

sample time history of the displacement measured by a transducer. Initial velocity, estimated by means of numerical derivation, is very close to zero.

## 2.2 Wall kinematics

Theoretically, the rocking wall shall be considered a single-degree-of-freedom oscillator. However, following the approach by Liberatore and Spera (2001a), five transducers are used in order to check if additional degrees of freedom are activated. The five instruments (Fig. 5, no. 0–4) make it possible to check if the motion is just a rotation.

Given the geometric parameters and the global coordinate axes in Fig. 7a, the time-varying total length (initial, $l$, + variation, $\Delta l$) of the $i$-th transducer can be expressed as a function of the degrees of freedom of the wall. Four degrees of freedom are contemplated (Fig. 7b). With reference to the centre of the base: $v, w$ = displacement parallel to $x, y$ axis, $\phi$ = rotation around the $z$ axis; additionally: $\theta$ = rotation around the $x$ axis passing through the

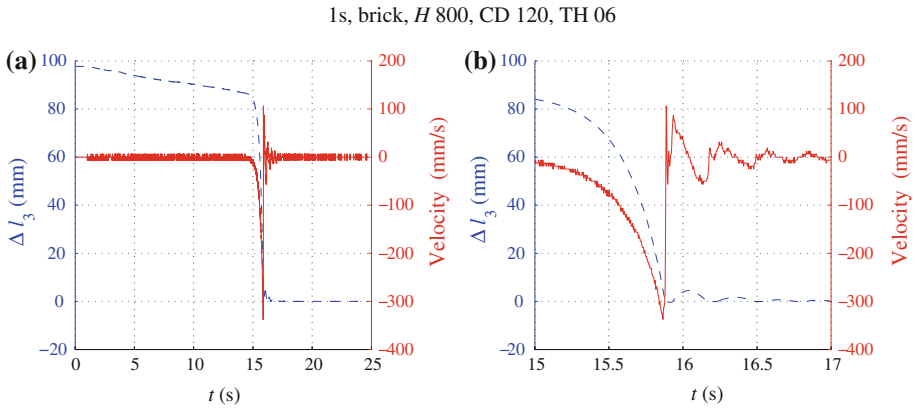


**Fig. 6** Sample time history record. Displacement, $\Delta l$, measured by transducer 3, dashed line, and velocity, solid line, obtained by means of numerical derivation. **b** is a zoom of **a** on the window of significant motion

relevant base corner. Considering the walls' geometric characteristics and the absence of any excitation, it has been postulated that complete uplift and rotation around $y$ axis do not occur.

Following the approach in Liberatore and Spera (2001a), for each of the five instruments, 0–4 (Fig. 7c), it is possible to state the following equation:

$$l_i + \Delta l_i = \left|\mathbf{u}_{i,7}\right| = \sqrt{\left(\sum_{j=1}^{6} u_{i,j}^{x}\right)^2 + \left(\sum_{j=1}^{6} u_{i,j}^{y}\right)^2 + \left(\sum_{j=1}^{6} u_{i,j}^{z}\right)^2} \tag{3}$$

Assuming that the instruments are initially horizontal and anchored on the vertical symmetry axes of the two lateral faces, the vector components of Eq. (3), for transducers 0–3, are:

$$\mathbf{u}_{i,1} = \begin{cases} 0 \\ l_i \\ 0 \end{cases} \qquad \mathbf{u}_{i,2} = \begin{cases} 0 \\ -r_i \cdot s \cdot \cos\beta_i \\ -r_i \cdot \sin\beta_i \end{cases}$$

$$\mathbf{u}_{i,3} = \begin{cases} -f \cdot k \\ b \cdot s \\ 0 \end{cases} \qquad \mathbf{u}_{i,4} = \begin{cases} v \\ w \\ b \cdot \sin|\theta| \end{cases}$$

$$\mathbf{u}_{i,5} = \begin{cases} f \cdot k \cdot \cos\phi + b \cdot s \cdot \sin\phi \cdot \cos\theta \\ f \cdot k \cdot \sin\phi - b \cdot s \cdot \cos\phi \cdot \cos\theta \\ -b \cdot \sin|\theta| \end{cases} \qquad \mathbf{u}_{i,6} = \begin{cases} -r_i \cdot s \cdot \cos(\beta_i + |\theta|) \cdot \sin\phi \\ +r_i \cdot s \cdot \cos(\beta_i + |\theta|) \cdot \cos\phi \\ r_i \cdot \sin(\beta_i + |\theta|) \end{cases} \tag{4}$$

$$k = \begin{cases} -1, & i = 0,\ 1 \\ +1, & i = 2,\ 3 \end{cases}$$

$$s = \begin{cases} \operatorname{sgn}(\theta), & \theta \neq 0 \\ \operatorname{sgn}\left(\dot{\theta}\right), & \theta = 0 \end{cases}$$

with geometrical parameter $f$ shown in Fig. 7a, and $l_i$, $r_i$, $\beta_i$ shown in Fig. 7d for the $i$-th transducer. The sums of the components in the right hand side of Eq. (3) can be simplified in the following equations:

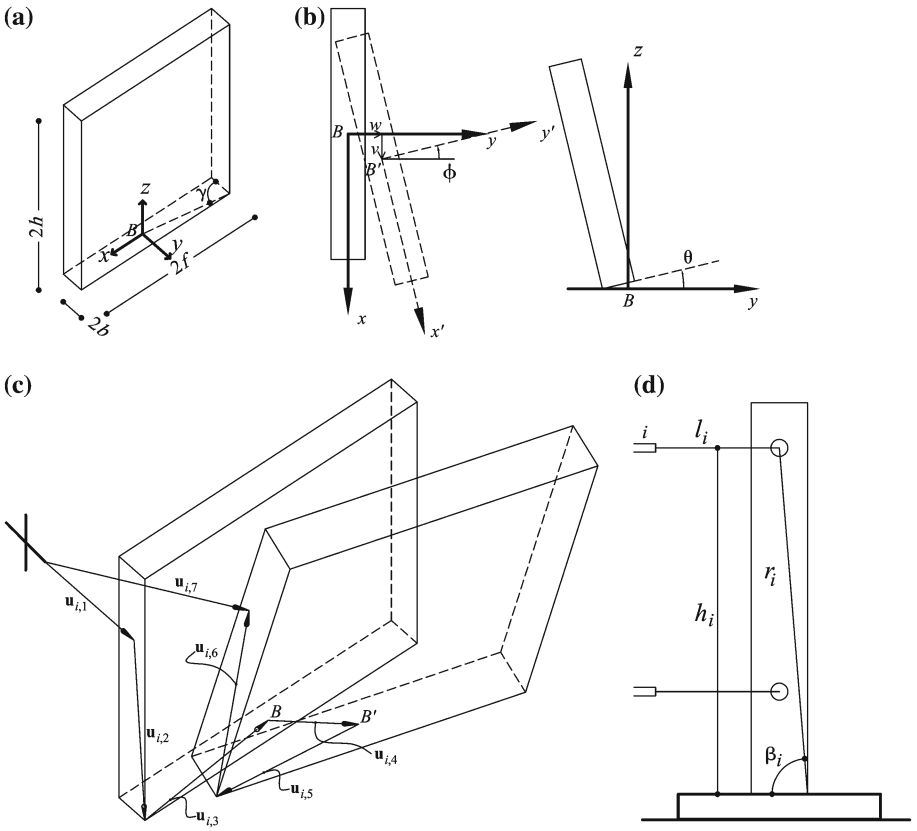


**Fig. 7** Geometric and kinematic parameters of the rocking façade: **a** geometry and global axes; **b** *xy*, *yz* plan kinematics; **c** displaced configuration of the façade and vectors, $u_{i,j}$, related to the variation of length of the displacement transducer; **d** geometric parameters of the $i$-th instrument

$$\begin{aligned}
\sum_{j=1}^{6} u_{i,j}^{x} &= v + f \cdot k \cdot (\cos\phi - 1) + r_i \cdot s \cdot \sin\phi \cdot \sin\beta_i \cdot \sin|\theta| \\
\sum_{j=1}^{6} u_{i,j}^{y} &= l_i + w + f \cdot k \cdot \sin\phi - r_i \cdot s \cdot \cos\phi \cdot \sin\beta_i \cdot \sin|\theta| \\
\sum_{j=1}^{6} u_{i,j}^{z} &= r_i \cdot [\sin(\beta_i + |\theta|) - \sin\beta_i]
\end{aligned} \tag{5}$$

For the 4-th transducer only $\mathbf{u}_{i,1}$ changes in Eq. (4):

$$\mathbf{u}_{4,1} = \begin{cases} -l_4 \\ 0 \\ 0 \end{cases} \tag{6}$$

with $k = 1$ in $u_{4,3}$ and $u_{4,5}$. Accordingly, the first two expressions in Eq. (5) become:

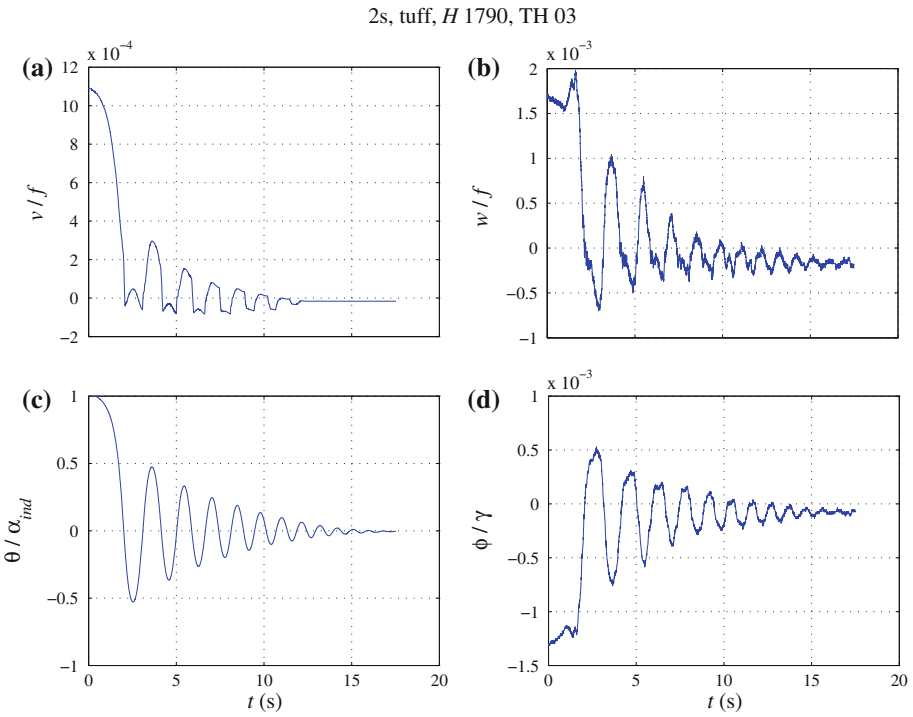


**Fig. 8** Sample time history computed by solving the system of four non linear equations obtained from Eq. (3). $t =$ time. Normalised degrees of freedom (Fig. 7): **a** displacement parallel to $x$ axis; **b** displacement parallel to $y$ axis; **c** rotation around $x$ axis, $\alpha_{ind}$ = reduced value of the angle $\alpha$ in order to take into account the indenting of the mortar with respect to the unit face, and the building tolerances of the wall along the height; **d** rotation around $z$ axis

$$\begin{aligned}\sum_{j=1}^{6} u^{x}_{4,j} &= -l_4 + v + f \cdot (\cos\phi - 1) + r_4 \cdot s \cdot \sin\phi \cdot \sin\beta_4 \cdot \sin|\theta| \\ \sum_{j=1}^{6} u^{y}_{4,j} &= w + f \cdot \sin\phi - r_4 \cdot s \cdot \cos\phi \cdot \sin\beta_4 \cdot \sin|\theta|\end{aligned} \tag{7}$$

The four kinematic unknowns $v, w, \theta$, and $\phi$ are determined by numerically solving, for each time step, four non linear equations obtained from Eq. (3) by considering four instruments. Usually transducers 0–1, and 3–4 are used, leaving transducer 2 as backup for instrument malfunctioning. Angular velocity $\dot{\theta}$ has been numerically computed from angular displacement.

In Fig. 8 the time histories of the four degrees of freedom of a sample test are presented. It is evident that only the rotation out of plane $\theta$ (Fig. 8c) assumes significant values. Nonetheless, the maximum value of rotation, $\phi$, around the vertical axis is non zero, as observed also by Peña et al. (2007).

In the range of the $h/b$ ratios examined in this experimental campaign, rotation $\theta$ determined by solving the system of four nonlinear equations based on Eq. (3) is very similar to that determined using the following simplified expression:

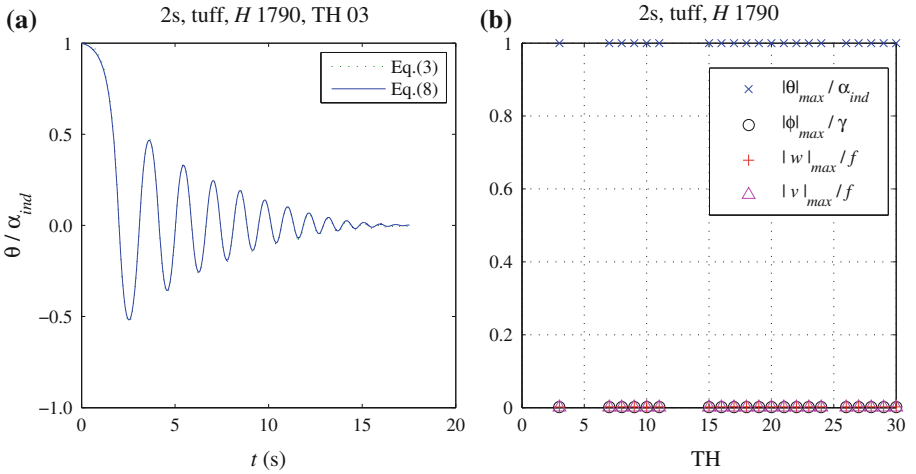


**Fig. 9** **a** Comparison between rotations θ determined solving the system of four non linear equations obtained from Eq. (3) and solving Eq. (8). The two curves are almost perfectly superimposed. **b** Normalised maximum absolute values of the four degrees of freedom for the time history tests, TH, on specimen no. 5a (Table 2)

$$\theta \cong \arctan\left(\frac{\Delta l_i}{h_i}\right) \tag{8}$$

with $h_i$ = height of the $i$-th transducer above the rocking hinge level, $i = 3, 5$. A comparison between the two rotations is presented in Fig. 9a.

The other kinematic parameters oscillate close to zero. Such oscillations and the residual figures are at least partially related to small vibrations at the anchorage of the transducer to the wall and to instrument tolerance. This behaviour was observed in most of the tests performed (Fig. 9b).

The absence of appreciable sliding is in agreement with what has been suggested at a theoretical level (Shenton 1996). According to this model, no sliding will occur during free oscillations if the static coefficient of friction, $\mu_s$, satisfies the following inequality:

$$\mu_s \geq \frac{3\varsigma}{1+4\varsigma^2} \tag{9}$$

Equation (9) is always satisfied if $\mu_s > b/h$. The largest value of $b/h$ of the walls tested is approximately 0.15, far below what is expected for the static coefficient of friction in the masonry, which usually falls within the 0.6–0.7 interval (Rankine 1863).

On the contrary, if forced oscillations are considered, sliding or slide-rotation is possible even if $\mu_s > b/h$, depending on the magnitude of the horizontal component of the ground acceleration $\ddot{x}_g$. This helps to explain why sliding and slide-rotations have been observed by other investigators in forced vibration tests on stockier blocks (Ageno and Sinopoli 1991).

The lack of noticeable sliding and the very limited damage accumulation, in terms of mortar crushing or loss of monolithicity, have made it possible to repeat the tests several times. Only in the case of one-sided rocking did the upper corners of the façade suffer progressive dislocations that finally prevented additional experimentation.

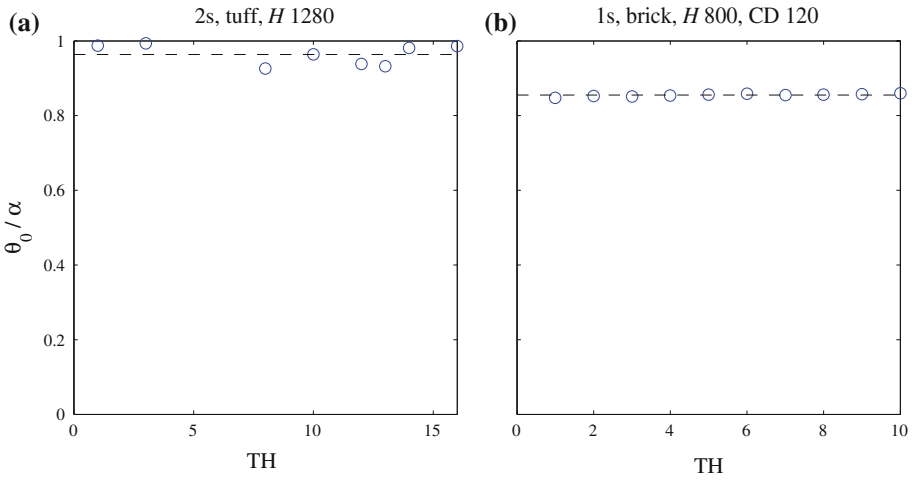


**Fig. 10** Ratio between initial rotation $\theta_0$ and nominal value of $\alpha(=\ \arctan\ (b/h)$, refer to Fig. 1), varying the time history, TH

## 3 Experimental estimation of energy dissipation

The experimental coefficient of restitution, $e_{exp}$, was estimated for each time history. The application of the initial displacement by means of the screw device has shown that the experimental instability displacement is usually smaller than the nominal instability displacement (Fig. 10). This phenomenon can be explained in terms of the local rounding of the rocking hinge, the indenting of the mortar with respect to the unit face, and the building tolerances of the wall along the height.

Once rotation $\theta$ was determined as explained in Sect. 2.2, and if the initial rotation had been applied with the screw device up to the instability threshold, rotation $\theta$ was normalised with respect to a reduced value of the angle $\alpha$, $\alpha_{ind} = \theta_0$, with $\theta_0$ = initial rotation. Based on the piece-wise linear formulation by Housner (1963), acceptable for slender rocking elements, $e_{exp}$ after $n$ impacts can be estimated according to the following equation:

$$e_{exp} = \sqrt[2n]{\frac{1-\left(1-\frac{|\theta_n|}{\alpha_{ind}}\right)^2}{1-\left(1-\frac{|\theta_0|}{\alpha_{ind}}\right)^2}} \tag{10}$$

with $|\theta_n|$ = maximum absolute rotation after the $n$-th impact. If $\alpha$ is used, instead of $\alpha_{ind}$, $e_{exp}$ is in average larger by 5 % in one-sided rocking, while in two-sided rocking it is larger by less than 0.5 %.

The values of $e_{exp}$ obtained by applying Eq. (10) to the tests here described coincide substantially with those obtained using the expression proposed by Peña et al. (2007), valid irrespective of the $h/b$ ratio:

$$e_{exp} = \sqrt[2n]{\frac{\cos(\alpha - |\theta_n|) - \cos\alpha}{\cos(\alpha - |\theta_0|) - \cos\alpha}} \tag{11}$$

with $\alpha = \alpha_{ind}$.

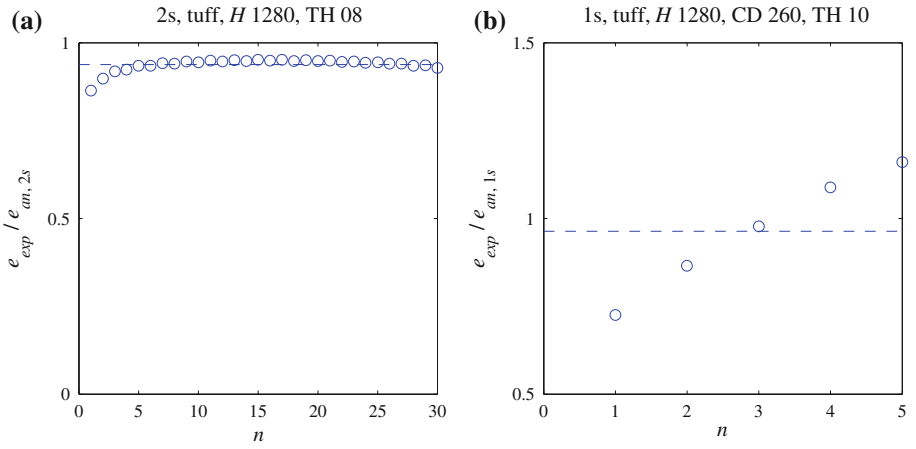


**Fig. 11** Ratio between experimental, $e_{exp}$, and analytic, $e_{an}$, coefficient of restitutions varying the number of impacts, $n$. **a** Two-sided rocking, 2s; **b** one-sided rocking, 1s; $e_{an,1s}$ is given in Eq. (14)

As shown by both Eqs. (10) and (11), the value of $e_{exp}$ can be affected by the number $n$ of impacts considered. In Fig. 11 this aspect is illustrated for both two-sided and one-sided rocking. In the first case, energy dissipation remains constant to a large extent throughout the time history. In one-sided rocking, on the other hand, energy dissipation is more markedly amplitude-dependent. Correspondingly, if the initial rotation is disregarded, the value of $e_{exp}$ does not change sensibly in two-sided rocking, while it is usually larger in one-sided rocking.

In Fig. 11a and in the rest of the paper, the value of $e_{exp}$, of a two-sided rocking test has been divided by $e_{an,2s}$ (Eq. 2) in order to obtain a comparison with a parameter which can be calculated for any given wall, even one that has not been tested. In calculating $e_{an,2s}$ a nominal value of $\alpha$ has been assumed. In this way $e_{an,2s}$ can be readily calculated, even if the rounding of the corner or the indenting of the mortar joint is not known. Moreover, even for the stockiest wall tested here, a 20% difference between $\alpha$ and $\alpha_{ind}$ yields a 1% difference in the value of $e_{an}$.

Equation (2) clearly does not apply to one-sided rocking. If impacts with the base and the transverse walls happen at the same time, and rotation around a corner continues with a simple change of sign, no rocking occurs, because no change in the hinge takes place. However, a different solution can be found if it is assumed that the impacts against the base and against the transverse walls happen in two close but separate instants. This is actually what happens if there is a gap between façade and transverse walls, as observed in shake table tests (Al Shawa et al. 2009). After the impact against the base, which involves an initial change in the rocking hinge, an impact against the upper corner can be hypothesised (Fig. 12). If the conservation of angular momentum is assumed, and one supposes that the impulse passes through this upper corner, it is possible to obtain the following expression of the analytic coefficient of restitution of the impact against transverse walls, $e_{an,tr}$:

$$e_{an,\,tr} = 1 - 2\frac{mR^2}{I_O}\cos^2\alpha \tag{12}$$

If the wall is homogeneous the previous equation becomes:

$$e_{an,\,tr} = 1 - \frac{3}{2}\cos^2\alpha = \frac{2-\varsigma^2}{2(\varsigma^2+1)} \tag{13}$$

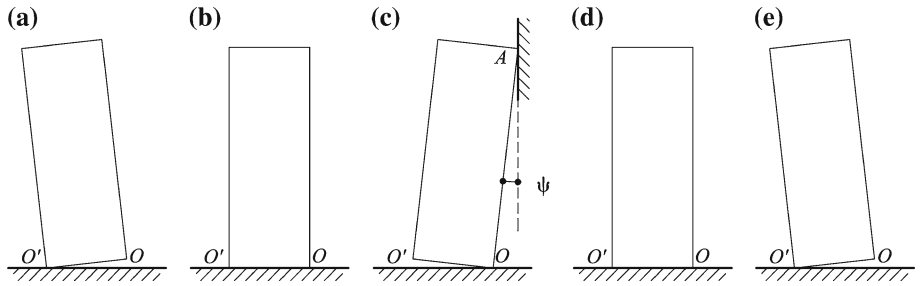


**Fig. 12** Model of the impact against the transverse walls as three separate impacts and as a rocking around the upper corner, *A*

It is worth noting that the equations are independent of the size of the gap between transverse walls and façade. This gap is practically inescapable, due either to construction tolerances or to the space left by the mortar in a previously filled vertical joint.

In the range of usual values of the aspect ratio, $e_{an,tr}$ is negative. Only for $\varsigma < \sqrt{2}$, does $e_{an,tr} > 0$. A negative value for the coefficient of restitution implies a rebound, which is what has been observed. Moreover, in the range of $h/b$ tested, ranging between 6.5 and 14.6, $e_{an,tr}$ varies between $-0.47$ and $-0.49$. Within the framework assumed, the size of the impact surface between façade and transverse walls is irrelevant. The tests performed also investigated this aspect by varying parameter CD.

After this impact, a third impact against the base can be assumed. Thus, in practical terms, in one sided rocking the impact can be modelled by multiplying the velocity by $e_{an,2s}$ twice and by $e_{an,tr}$ once. Thus, an analytic coefficient of restitution for one sided rocking, $e_{an,1s}$, can be defined as:

$$e_{an,1s} = \left(1 - \frac{3}{2}\sin^2\alpha\right)^2 \left(1 - \frac{3}{2}\cos^2\alpha\right) \tag{14}$$

In Fig. 11b, and in the rest of the paper, the value $e_{exp}$ of a one-sided rocking test has been divided by $e_{an,1s}$. It is evident that $|e_{an,1s}| << \quad e_{an,2s}$, and this is mainly due to $e_{an,tr}$.

In two-sided rocking, the value of the ratio between experimental and analytic coefficients of restitution, $e_{exp}/e_{an,2s}$, is less than one (Fig. 13a). As already observed (Fig. 11a), the results do not markedly depend on amplitude and they appear stable both within each test series and moving from one specimen to another. This is probably due to the presence of the mortar in the rocking hinge layer, which makes contact condition similar in all tests. Only one test series shows much smaller values for the ratio compared to all the others (Fig. 13a). If the entire time history is taken into consideration, and if this series is disregarded, the mean value of $e_{exp}/e_{an,2s}$ is approximately 0.95. If all series are considered, the ratio is smaller, being equal on average to 0.93. $e_{exp}/e_{an,2s} = 0.95$ can probably be taken as an approximate estimation of the coefficient of restitution in a parapet wall whose rocking stability has to be assessed by means of non-linear time history analyses. The ratio $e_{exp}/e_{an,2s}$ is close to one, irrespective of the aspect ratio of the wall. This means that Housner formulation of the coefficient of restitution, Eq. (2), shows the right trend with $h/b$, but underestimates energy damping. In Sect. 5 the influence of higher energy damping will be investigated.

In one-sided rocking, the results are more scattered compared to two-sided rocking (Fig. 13b). Unlike two-sided rocking, energy dissipation is amplitude-dependant: the larger the velocity, the larger the dissipation (and the smaller $e$, Table 3). As a rule of thumb, if we suppose that damping remains constant with amplitude, a coefficient of restitution of

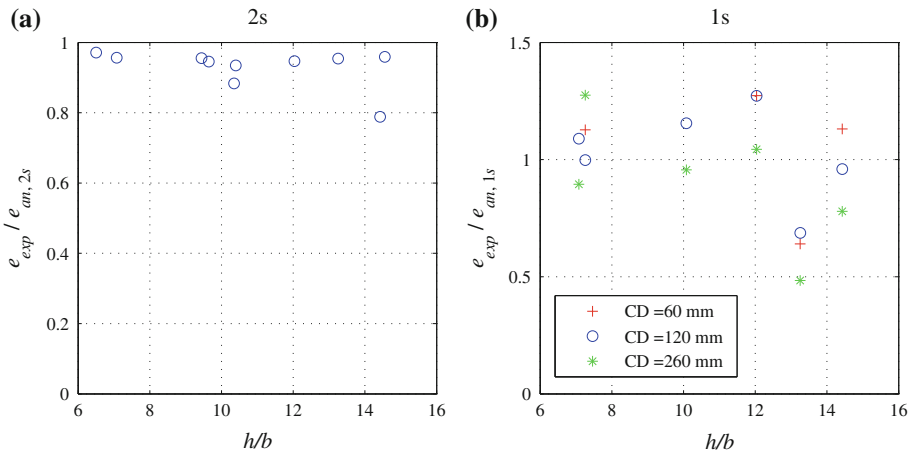


**Fig. 13** Ratio between experimental and analytic coefficients of restitution, $e_{exp}/e_{an}$, in each test series. Test series are identified by means of the aspect ratio, $h/b$. **a** Two-sided, 2s, and **b** one-sided, 1s, rocking. In **b** CD is the contact depth between façade and each of the transverse walls (Fig. 4)

**Table 3** One-sided rocking. Mean values of the ratio between experimental and analytic (Eq. 14) coefficients of restitution, $e_{exp}/e_{an,1s}$, considering different windows in the experimental time histories

| Complete | Disregarding the first half cycle | Considering only the first half cycle |
|---|---|---|
| 1.05 | 1.34 | 0.72 |

$1.05 e_{an,1s}$ may be assumed. An improvement is obtained if a linear relationship between non dimensional peak rotation before impact, $|\theta^-|/\alpha$, is assumed:

$$\frac{e_{exp}}{e_{an,\,1s}} = 1.17 - 0.453\frac{|\theta^-|}{\alpha} \tag{15}$$

However, when performing a forced-vibration non-linear time-history analysis, there is no peak rotation. Therefore, it is useful to express Eq. (15) in terms of velocity before impact, $\dot{\theta}^-$, obtained by equating kinetic and potential energies.

This velocity can be made non dimensional, considering the overturning velocity, $\dot{\theta}_r$, i.e. the velocity required to overturn a block at rest:

$$\dot{\theta}_r^2 = 2\frac{mgR}{I_O}(1-\cos\alpha) \tag{16}$$

with $g$ = gravity acceleration. Thus, Eq. (15) becomes:

$$\frac{e_{exp}}{e_{an,\,1s}} = 1.18 - 0.473\left(\frac{\dot{\theta}^-}{\dot{\theta}_r}\right)^2 \tag{17}$$

Nonetheless, there is a significant scatter in the experimental data, as the coefficient of determination is equal to 0.41.

The experimental coefficient of restitution remains stable test after test, within a test series. The unit material has no effect on the ratio $e_{exp}/e_{an,1s}$, and the ratio shows no clear trend with $h/b$.

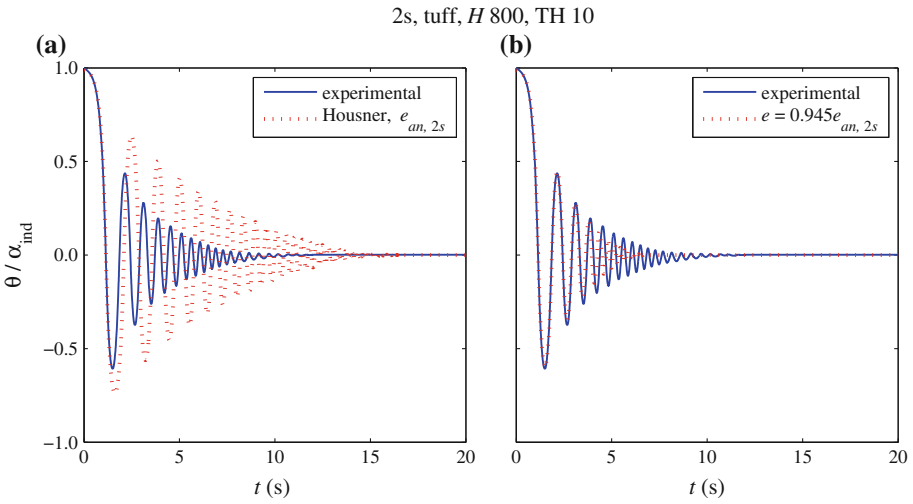


**Fig. 14** Two-sided rocking. Comparison between experimental and analytic time histories. **a** Literature models; **b** experimentally calibrated models. Due to numerical sensitivity issues, all analytic models assume $\theta_0 / \alpha = 0.985$

The size of the contact surfaces between façade and transverse walls, measured by contact depth CD (Fig. 4), has no systematic influence on energy damping. Therefore, it may be assumed that the analytic model of Eq. (14) is qualitatively correct. However, it is reasonable to assume that a minimum amount of contact depth is necessary in order to avoid material failure at impacts.

It is worth noting that the experimental coefficient of restitution in one-sided rocking, although much lower than in two-sided rocking, is not zero as tentatively suggested by Liberatore and Spera (2003). As a matter of fact, the two researchers themselves regarded this assumption as probably being over-optimistic. On the basis of the tests presented here, it may be stated that numerical analyses performed assuming $e_{an,1s} = 0$ are unsafe, as shown in Sect. 5.

If the analytic coefficient of restitution for two-sided rocking (Eq. 2) is used to reproduce experimental time histories, poor results are obtained (Fig. 14a). On the other hand, an experimentally calibrated coefficient of restitution markedly enhances agreement (Fig. 14b). The still-not-perfect match may be partially due to the amplitude dependency of the $e_{exp}/e_{an,2s}$ ratio, which is present, albeit weak, and to the lack of symmetry of the actual wall. A better match has been obtained using a three-branch moment-rotation relationship (Doherty et al. 2002; Sorrentino et al. 2008a), but using the same experimentally calibrated coefficient of restitution.

The same comparison was performed for one-sided rocking (Fig. 15a). Here it may be observed that the analytic coefficient of restitution of Eq. (14) is a marked improvement on the ones proposed in the literature, which either underestimate (Hogan 1992) or overestimate (Liberatore and Spera 2003) energy damping. The agreement between experimental and analytic time histories is improved if the analytic coefficient of restitution is experimentally calibrated or made amplitude dependant (Fig. 15b). The still not perfect match may be related to the presence of negative rotations, due to the gap existing between façade and transverse walls. Therefore, the last portion of the experimental time history features small-amplitude two-sided rocking, which the analytical model of one-sided rocking is not able to reproduce.

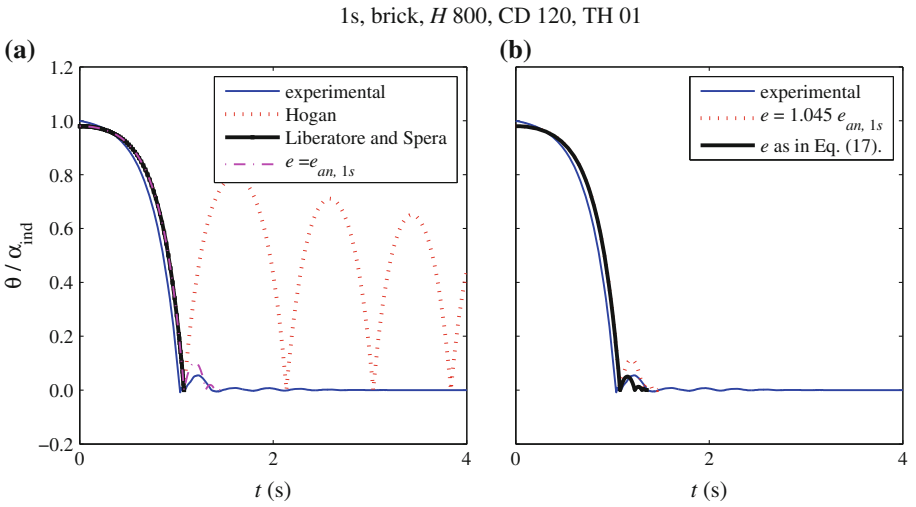


**Fig. 15** One-sided rocking. Comparison between experimental and analytic time histories. **a** Literature and analytic models; **b** experimentally calibrated models

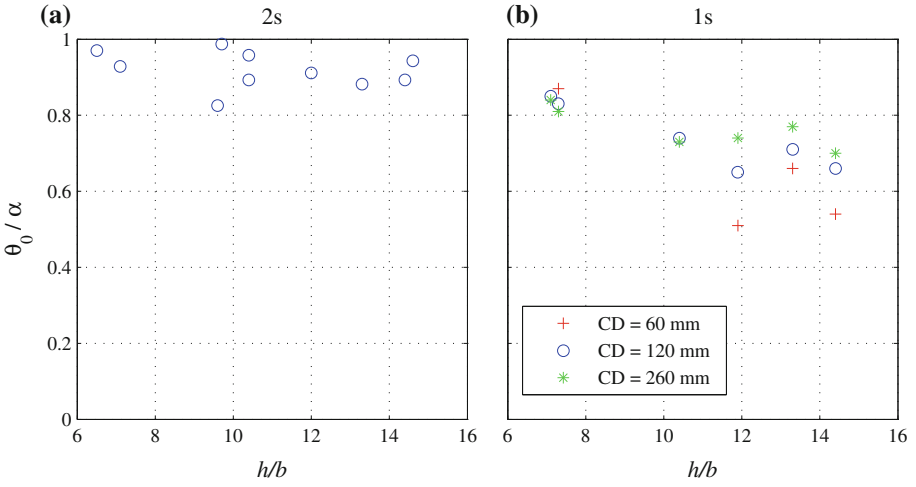


**Fig. 16** Mean values of ratio between initial (instability) rotation angle $\theta_0$ and nominal angle $\alpha$ (Fig. 1), in each test series

## 4 Additional experimental parameters

In addition to the experimental coefficient of restitution, the response of the walls tested was investigated by observing several parameters, presented here as mean values of each test series.

The non-dimensional initial rotation is rather stable in a single test series (Fig. 10), even in the case of the heaviest walls tested. However, it can be significantly scattered from wall to wall, and from test series to test series. This is true for both two-sided and one-sided rocking experiments, although the initial rotation is usually larger in two-sided rocking than in

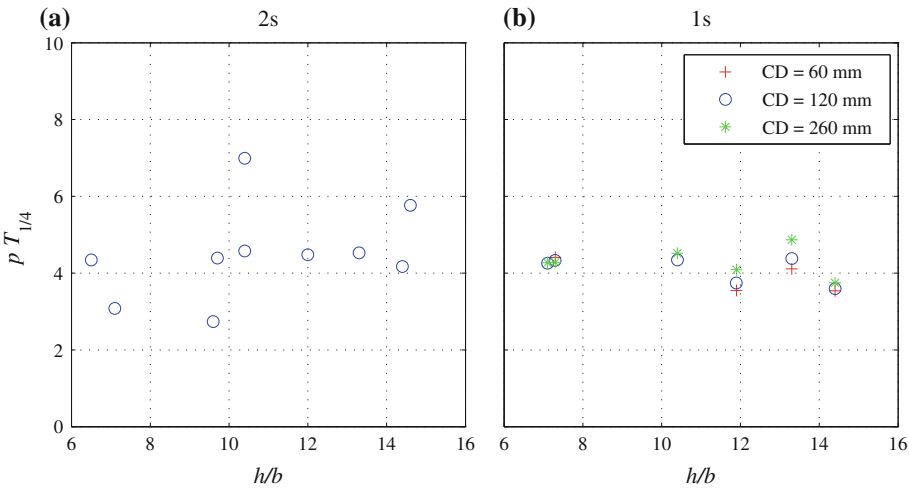


**Fig. 17** For each test series, mean values of non-dimensional period of the wall, $T_{1/4}$, of the first quarter cycle of the time history multiplied, as in Housner (1963), by the frequency parameter $p = \sqrt{mgR/I_O}$

one-sided rocking (Fig. 16). Such behaviour is probably due to mortar debris accumulation in the rocking hinge layer, not only during rocking but also when changing test setup. As a matter of fact, when the hinge layer was cleaned between two test series, the initial rotation increased (Decanini et al. 2009). Mean non-dimensional initial rotation $\theta_0 / \alpha$ is 0.91 in two-sided rocking and 0.73 in one-sided rocking.

The non-dimensional period of the wall, with reference to the first quarter of the first cycle, is usually close to or larger than 4 (Fig. 17), indicating a non-dimensional initial rotation close to one (Housner 1963). A larger scatter in the initial period may be observed in two-sided rocking. As suggested by theoretical considerations (Housner 1963; Sorrentino et al. 2008b), the period is amplitude-dependant (Figs. 6, 9a). As already observed in the case of non-dimensional initial rotation, the non-dimensional period of the first quarter of the first cycle is usually stable in each test series.

The number of cycles of each test series can be very scattered (Fig. 18). This must be due to the very small amplitude of the last oscillations, the imperfection of the rocking hinge, and so on. Contrary to what has been observed about nondimensional initial rotations and period, the scatter in the number of peaks may be observed even within a single test series. The number of cycles is of course higher in two-sided rocking, because the system is less damped.

Considerations similar to those developed regarding the number of cycles apply to the non-dimensional duration of free rocking (Fig. 19).

In two test series of two-sided rocking, the symmetry of the specimen response was investigated by pushing the wall in a test and by pulling the wall in the following test. With reference to the mean initial rotation measured when pushing the specimen, when pulling the wall the initial rotation changes by 13% in one case and by and 3% in the other. The coefficient of restitution varies by 2 and by 4% respectively, if the entire time history is considered. Such changes may be related to the tests previously performed both on the walls and on building tolerances. In the rest of the paper, symmetric behaviour has always been assumed.

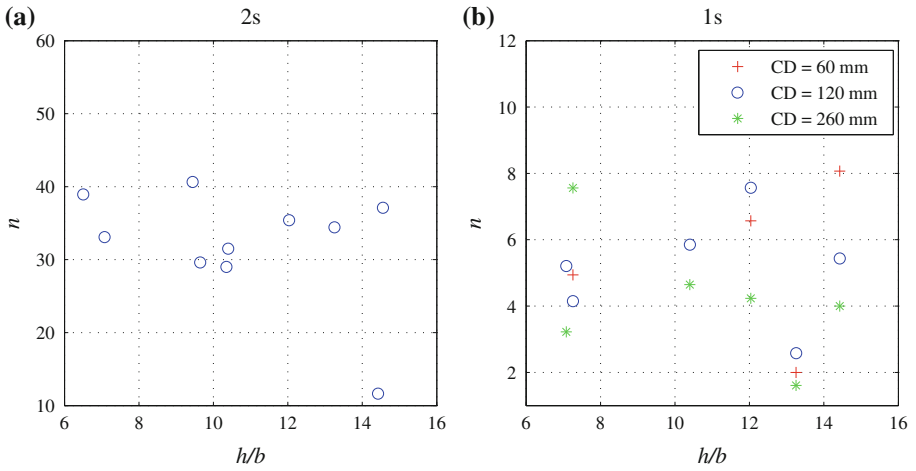


**Fig. 18** Number of cycles, $n$, in each test series. The scale of $y$-axis is different in **a** and **b**

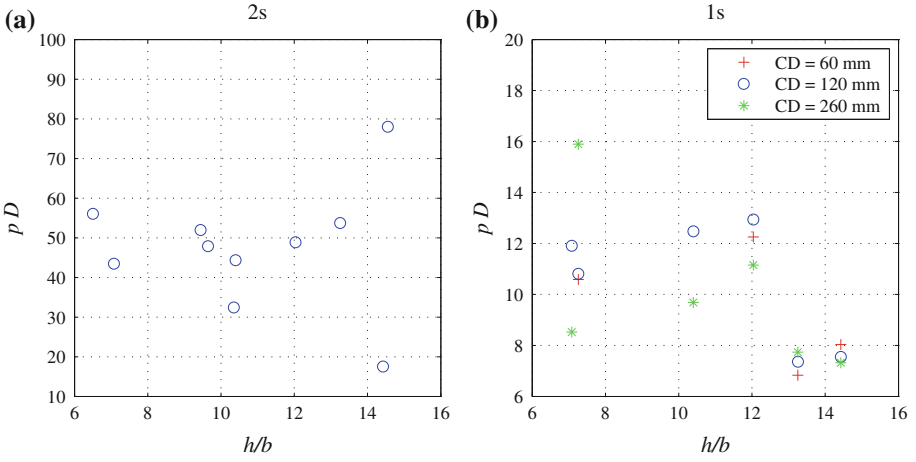


**Fig. 19** Non dimensional duration, $pD$, of free rocking in each test series. The scale of $y$-axis is different in **a** and **b**

Finally, the possible amplification of out-of-plane motion, due to deformation, was investigated. The displacement time history at the centre of the wall, measured by instrument no. 5 (Fig. 5), was compared to displacement at the same height of the same instrument, obtained from rotation θ. This comparison is presented in Fig. 20, for both a sample time history and a complete test series. In the case of the test series, the maximum displacements after the first impact are compared. The ratio between such top rates oscillates around 1, with mean value of 1.01 for CD = 60 mm, and mean value of 1.05 for CD = 260 mm. Because maximum displacements are in the order of a few millimetres, the wall's maximum deformation is a fraction of a millimetre and about 1/5000 of specimen length.

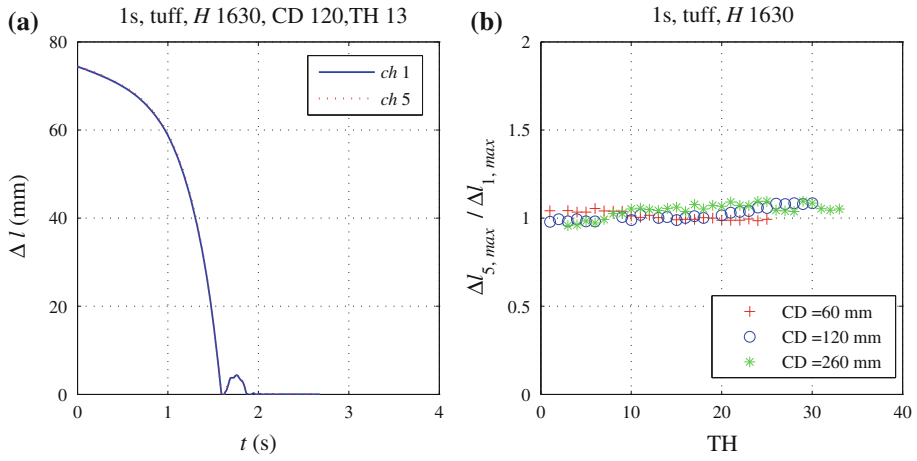


**Fig. 20** Amplification of out-of-plane displacement at the centre of the wall due to impact against transverse walls. **a** Sample time histories of displacement at the side and at the centre of the façade. **b** Ratio between maximum displacements at the side and at the centre of the façade, after the first impact, for a test series

## 5 Influence of the coefficient of restitution upon earthquake performance of rocking walls

The influence of a more accurate estimation of energy dissipation upon the earthquake performance of rocking walls was appraised by means of numerical analyses. The numerical procedure has been validated elsewhere (Sorrentino et al. 2006a).

First of all, the response of a two-sided rocking façade was studied in terms of overturning maps (Plaut et al. 1996; Sorrentino et al. 2006b). Each overturning map plots the response of a wall excited by a recorded accelerogram. Each point of a map represents the overturning (gray) or non overturning (white) of the wall for the selected accelerogram whose amplitude, $A$, has been scaled to $A_S$, and whose duration, $D$, has been scaled to $D_S$. The scaling of the signal can be interpreted as a scaling of the wall. The response of the selected wall to a signal with amplitude scaled by $A_S/A$, is equal, according to Housner (1963) piece-wise linear model, to the response of wall whose $\alpha$ is scaled by $A/A_S$. This is to say that increasing the amplitude of the record is equivalent to increasing the geometric slenderness of the wall. The response of the selected wall to a signal with duration scaled by $D_S/D$, is equal to the response of a wall whose $R$ is scaled by $(D/D_S)^2$. Therefore, an increased duration of the accelerogram is equivalent to reducing the size of the wall in a non-linear fashion.

201 discrete values of amplitude and duration are considered, scaled to between 50 % and 150 % of natural values. Thus, each map is the result of 40401 time histories. 20 accelerograms were used, whose main features are reported in Table 4.

Figure 21a illustrates a sample map computed in Sorrentino et al. (2006b), where $e = e_{an,2s}$ (Eq. 2). The boundary between overturning and non overturning domains has a non-smooth, non-connected shape.

In Fig. 21b the same map is computed for $e = 0.95\ e_{an,2s}$. As could have been expected, the number of overturnings decreases.

If this comparison is performed for all of the 20 accelerograms considered, Fig. 22a shows that the reduction of the coefficient of restitution can have a varying effect on the number of overturnings, $N_O$. This phenomenon may be related to the time of occurrence of the

**Table 4** Recorded accelerograms used and their main features

| | Event | Date | $M_W$[a] | Station | Record | $d$[b] (km) | PGA[c] (g) | PGV[c] (cm/s) | $D$[d] (s) |
|---|---|---|---|---|---|---|---|---|---|
| 1 | Imperial Valley, CA, USA | 1940-V-19 | 7.0 | El Centro Array #9 | 40ElC180 | 6.4 | 0.35 | 29.8 | 53.8 |
| 2 | Kern County, CA, USA | 1952-VII-21 | 7.4 | Taft Lincoln School | Taft111 | 40 | 0.18 | 17.5 | 54.4 |
| 3 | San Fernando, CA, USA | 1971-II-9 | 6.6 | Pacoima Dam, abutment | Pac164 | 3.2 | 1.17 | 114.4 | 41.78 |
| 4 | Friuli, Italy | 1976-V-6 | 6.5 | Tolmezzo | TolmezWE | 16 | 0.35 | 30.8 | 36.5 |
| 5 | Romania | 1977-III-4 | 7.5 | Bucarest, Romania Building Research Institute | Bucar0 | 150 | 0.21 | 73.6 | 16.2 |
| 6 | Imperial Valley, CA, USA | 1979-X-15 | 6.5 | Bonds Corner | BCr230 | 2.8 | 0.78 | 45.9 | 37.595 |
| 7 | Imperial Valley, CA, USA | 1979-X-15 | 6.5 | El Centro Array #7 | IVC230 | 0.2 | 0.46 | 109.3 | 36.795 |
| 8 | Michoacan, Mexico | 1985-IX-19 | 8.1[e] | Secretaria comunicacion and tran. Texcoco lake bed zone | SecreN27 | 389 | 0.17 | 59.8 | 135.2 |
| 9 | Nahanni, Canada | 1985-XII-23 | 6.8 | Site 1 | 1St280 | 0.1 | 1.10 | 46.1 | 20.545 |
| 10 | Loma Prieta, CA, USA | 1989-X-18 | 6.9 | Los Gatos Presentation Center | LGPC000 | 0.1 | 0.56 | 94.8 | 24.95 |
| 11 | Landers, CA, USA | 1992-VI-28 | 7.3 | Joshua Tree Fire Station | Joshua90 | 11.3 | 0.28 | 43.2 | 80 |
| 12 | Landers, CA, USA | 1992-VI-28 | 7.3 | Lucerne Valley | LucN80W | 1.8 | 0.64 | 146.5 | 40 |
| 13 | Northridge, CA, USA | 1994-I-17 | 6.7 | Rinaldi Receiving Station | RRS228 | 0.1 | 0.84 | 166.1 | 14.945 |
| 14 | Northridge, CA, USA | 1994-I-17 | 6.7 | Sylmar - Olive View Med Parking Lot Free Field | Syl360ff | 2 | 0.84 | 129.6 | 39.98 |
| 15 | Northridge, CA, USA | 1994-I-17 | 6.7 | Sylmar - Olive View Med Chan 63$^{rd}$ floor W wall | Syl360VI | 2 | 0.93 | 123.2 | 39.98 |
| 16 | Northridge, CA, USA | 1994-I-17 | 6.7 | Los Angeles - Hollywood Storage Grounds | LAHol0ff | 23.7 | 0.39 | 22.4 | 59.98 |
| 17 | Northridge, CA, USA | 1994-I-17 | 6.7 | Los Angeles - Hollywood Storage Bldg. Chan 48$^{th}$ floor center | LAHol0IV | 23.7 | 0.32 | 24.5 | 59.98 |
| 18 | Kobe, Japan | 1995-I-16 | 6.9 | KJMA | KJM000 | 1 | 0.82 | 81.3 | 47.98 |
| 19 | Kobe, Japan | 1995-I-16 | 6.9 | Takatori | Tak000 | 1.8 | 0.61 | 127.1 | 40.95 |
| 20 | Kocaeli, Turkey | 1999-VIII-17 | 7.4 | Yarimca Petrokimya Tesisleri | YPT330 | 2.6 | 0.35 | 62.2 | 34.995 |

[a] Moment magnitude
[b] Distance from the surface projection of the source
[c] Peak Ground: $PGA$ acceleration, $PGV$ velocity
[d] Duration
[e] Surface waves magnitude

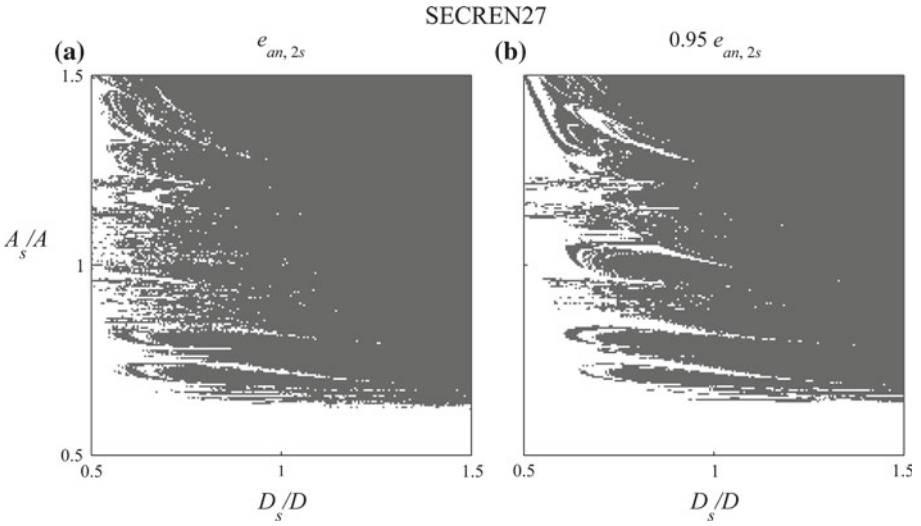


**Fig. 21** Overturning map for a two-sided rocking block ($\alpha = 0.1$ rad, $R = 3$ m, Fig. 1). **a** $e = e_{an,2s}$ (Sorrentino et al. 2006b); **b** $e = 0.95e_{an,2s}$. Overturned façades are represented by *gray dots*. For record details refer to Table 4

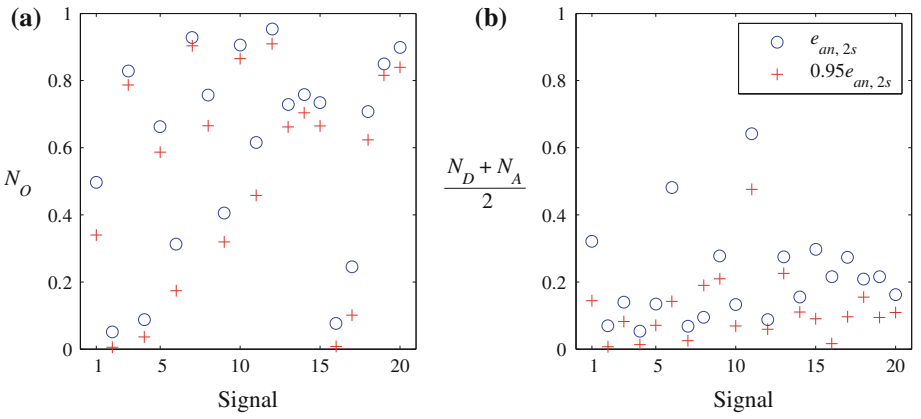


**Fig. 22** **a** Normalised number of overturnings, $N_O$, **b** Average normalised number of changes overturning–no overturning scaling duration and amplitude for 20 natural signals (Table 4), for $e = e_{an,2s}$ (Sorrentino et al. 2006b) and for $e = 0.95e_{an,2s}$

overturning. If such critical response is obtained due to an initial excitation pulse, an increase in the energy dissipated through impact is irrelevant, because no impact has occurred. However, if the overturning occurs after a few impacts, a reduced value of $e$ plays a role, because the wall will have a smaller velocity after hitting the base. On average, in the 20 maps computed, the reduction in the number of overturnings was equal to 25 %, with a minimum of 3 % and a maximum of 89 %.

Another aspect that Fig. 21 reveals is that the reduction of $e$ reduces the scatter of the response as well. In order to measure the scatter of the response in each map, two numerical indexes were defined: $N_D$ and $N_A$. These are the number of changes (overturning-no overturning), scaling up the duration and the amplitude respectively, normalised by the number of

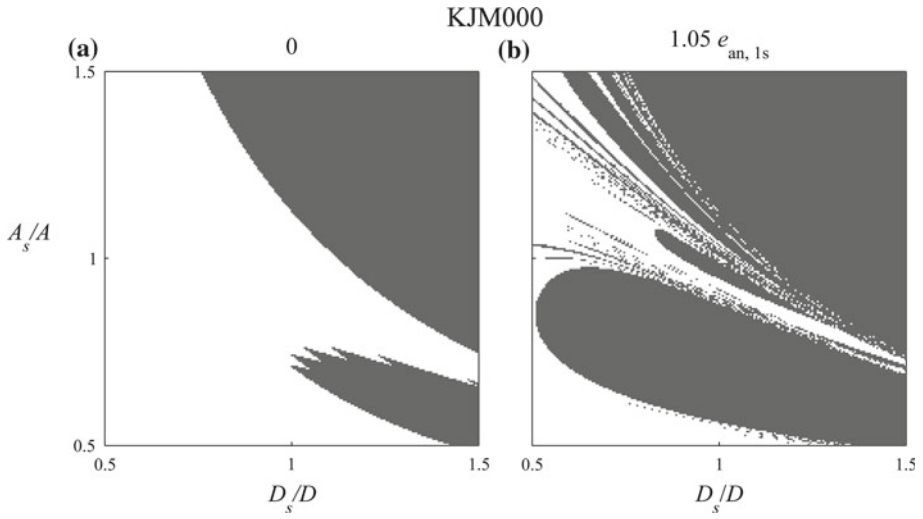


**Fig. 23** Overturning map for a one-sided rocking block ($\alpha = 0.1$ rad, $R = 3$ m, Fig. 1). **a** $e = 0$; **b** $e = 1.05e_{an,1s}$. Overturned façades are represented by *gray dots*. For record details refer to Table 4

overturnings (in order to take into account how many changes were actually possible). In Fig. 22b the average of $N_D$ and $N_A$ is presented for both the analytic (a) and the experimentally calibrated (b) coefficient of restitution. The response appears more ordered in the second case. On average, in the 20 maps computed, the reduction of scatter (as previously defined) was equal to 43 %. Therefore, increased energy dissipation not only reduces the overturning of a wall, but also makes its assessment more robust.

With reference to the same set of 20 natural accelerograms, overturning maps of a one-sided rocking wall were computed. Such maps have a shape similar to that already observed for two-sided rocking. In Fig. 23 the comparison is performed between a zero coefficient of restitution, and an experimentally calibrated coefficient of restitution. From such comparison it is clear that the first assumption is unsafe. In one-sided rocking, a reduction of $e$ might be relevant in one direction of rotation, but not in the other. The explanation of this performance is similar to that given for two-sided rocking. In one direction an initial pulse of the excitation might push the façade against the transverse walls, whereas in the other it might induce an overturning without previous significant impacts.

## 6 Conclusions

In this paper the role of energy damping on the earthquake performance of unreinforced-masonry rocking mechanisms has been evaluated. An experimental campaign considered the influence of several parameters on energy dissipation, measured by means of the so-called coefficient of restitution. Two boundary conditions have been taken into account: two-sided rocking (typical of a parapet wall) and one-sided rocking (façade adjacent to transverse walls). The experimental estimation of the coefficient of restitution was compared to the analytical coefficient of restitution.

In the case of two-sided rocking this coefficient is well known in the literature. The ratio between experimental and analytic coefficients is approximately 0.95. This 5% difference,

apparently negligible, has important consequences. First of all the accuracy of the reproduction of experimental time histories is markedly increased. Secondly, a reduced coefficient of restitution significantly reduces the number of overturnings and the scatter of the response.

In the case of one-sided rocking, an analytic coefficient of restitution was suggested. The coefficient was obtained following an impulsive mechanics approach. According to this approach the coefficient is not dependant on the size of the contact surface between façade and transverse walls. The tests confirmed this somewhat unexpected behaviour. In one-sided rocking, unlike two-sided rocking, energy damping is markedly amplitude-dependant. Therefore, in addition to an average ratio between experimental and analytical coefficients of approximately 1.05, a quadratic formulation with non-dimensional velocity at impact has been proposed.

In both two-sided and one-sided rocking, neither the material of the units nor the height-to-thickness ratio play any systematic role. The behaviour of the specimens is rather stable when the tests are repeated.

Other experimental parameters have also been considered. Displacement capacity is always smaller than what might be estimated based on geometry alone, and it is sensitive to imperfection in the rocking hinge. With reference to the tests performed, experimental displacement capacity is equal on average to 91% of geometrical value in two-sided rocking, while in one-sided rocking it is on average equal to 73%. However, such capacity remains fairly stable within a single test series. The same happens to the period of the first quarter of cycle. On the contrary, number of impacts and duration of rocking can be very scattered.

A kinematic formulation accounting for four possible degrees of freedom has shown that rocking rotation accounts for most of the motion, and sliding displacements are negligible. However, this conclusion might be attenuated if forced vibrations, stockier blocks, and different materials at interface are considered.

Finally, the numerical analyses performed have shown the importance of an accurate estimation of energy dissipation in order to take advantage of time history analyses in the seismic assessment of local collapse mechanisms in unreinforced masonry structures. Such refined estimation of energy dissipation shall also be considered when calibrating equivalent static procedures based on non-linear time history analysis.

**Acknowledgments** This work has been partially carried out under the program "Dipartimento di Protezione Civile—Consorzio RELUIS", signed on 2009-09-24 (no. 823), Thematic Area 1, Research Line 1, Task 1. The contribution of architect Stefano Benedetti, for the assistance during the laboratory tests, is kindly acknowledged. The authors wish to thank an anonymous reviewer for the careful reading of the manuscript and for his/her valuable suggestions.

## References

Ageno A, Sinopoli A (1991) Indagine teorica e sperimentale sul problema dell'urto tra blocchi rigidi. 5 Convegno Nazionale "L'Ingegneria Sismica in Italia", Palermo, 29 Settembre–2 Ottobre 1991

Al Shawa O, Benedetti S, Bellisario M, de Felice G, Mauro A, Paolacci F, Ranieri N, Roselli I, Sorrentino L (2009) Prove sperimentali su tavola vibrante di pareti murarie sollecitate fuori dal piano. ReLUIS final deliverable, Annex PF-1.2-UR09_15

Aslam M, Godden WG, Scalise T (1980) Earthquake rocking response of rigid bodies. J Struct Div-ASCE 106:377–392

Augenti N, Parisi F (2009) Experimental data analysis on mechanical parameters of tuff masonry. Workshop on design for rehabilitation of masonry structures, Wondermasonry, Lacco Ameno, 8–10 October 2009

Bernardini, A, Mattone R, Modena C, Pasero G, Pavano M, Pistone G, Roccati R, Zaupa F (1984) Determinazione delle capacità portanti per carichi verticali e laterali di pannelli murari in tufo.2 Convegno ASSIRCCO, Ferrara, 30 maggio–2 giugno 1984

Binda L, Mirabella Roberti G, Tiraboschi C (1996) Problemi di misura dei parametri meccanici della muratura e dei suoi componenti. La meccanica delle murature tra teoria e progetto, Messina, 18–20 settembre 1996
D'Ayala D, Speranza E (2003) Definition of collapse mechanisms and seismic vulnerability of historic masonry buildings. Earthq Spectra 19:479–509. doi:10.1193/1.1599896
Decanini LD, Gavarini C, Mollaioli F (2000) Some remarks on the Umbria-Marche earthquakes of 1997. Eur Earthq Eng 14:18–48
Decanini L, De Sortis A, Goretti A, Langenbach R, Mollaioli F, Rasulo A (2004) Performance of masonry buildings during the 2002 Molise, Italy, Earthquake. Earthq Spectra 20:S191–S220. doi:10.1193/1.1765106
Decanini LD, Masiani R, Al Shawa O, Benedetti S, Sorrentino L (2009) Prove sperimentali di dondolamento libero di pareti murarie. Rapporto conclusivo. ReLUIS 3rd year report, Annex 1.2-UR15-4
De Lorenzis L, DeJong M, Ochsendorf J (2007) Failure of masonry arches under impulse base motion. Earthq Eng Struct Dyn 36:2119–2136. doi:10.1002/eqe.719
Doherty KT, Griffith MC, Lam NTK, Wilson JL (2002) Displacement-based seismic analysis for out-of-plane bending of unreinforced masonry walls. Earthq Eng Struct Dyn 31:833–850. doi:10.1002/eqe.126
Goretti A, De Matteis U, Liberatore D (2007) Analisi sismica delle mura storiche di Camerino. 12 Convegno nazionale "L'ingegneria sismica in Italia", Pisa, 10–15 Giugno 2007
Griffith MC, Magenes G, Melis G, Picchi L (2003) Evaluation of out-of-plane stability of unreinforced masonry walls subjected to seismic excitation. J Earthq Eng 7:141–169. doi:10.1142/S1363246903000997
Griffith MC, Lam NTK, Wilson JL, Doherty KT (2004) Experimental investigation of URM walls in flexure. J Struct Eng-ASCE 130:423–432. doi:10.1061/(ASCE)0733-9445(2004)130:3(423)
Hogan SJ (1992) On the notion of a rigid block, tethered at one corner, under harmonic forcing. Proc R Soc Lon Ser-A 439:35–45
Housner GW (1963) The behavior of inverted pendulum structures during earthquakes. Bull Seismol Soc Am 53:403–417
Lagomarsino S, Resemini S (2009) The assessment of damage limitation state in the seismic analysis of monumental buildings. Earthq Spectra 25:323–346. doi:10.1193/1.3110242
Lam NTK, Wilson JL, Hutchinson GL (1995) The seismic resistance of unreinforced masonry cantilever walls in low seismicity areas. Bull New Zealand Natl Soc Earthq Eng 28:179–195
Lam NTK, Griffith MC, Wilson JL, Doherty KT (2003) Time–history analysis of URM walls in out-of-plane flexure. Eng Struct 25:743–754. doi:10.1016/S0141-0296(02)00218-3
Liberatore D, Spera G, D'Alessandro G, Nigro D (2002) Rocking of slender blocks subjected to seismic motion of the base. 12 European conference on earthquake engineering, London, 9–13 September 2002
Liberatore D, Spera G (2001a) Response of slender blocks subjected to seismic motion of the base: description of the experimental investigation. 5 international symposium on computer methods in structural masonry, Rome, 18–21 April 2001
Liberatore D, Spera G (2001b) Response of slender blocks subjected to seismic motion of the base: experimental results and initial numerical analyses. 5 international symposium on computer methods in structural masonry, Rome, 18–21 April 2001
Liberatore D, Spera G (2003) Analisi strutturale e intervento di consolidamento. In: Scalora G (ed) I tessuti urbani di Ortigia. Un metodo per il progetto di conservazione. Ente Scuola Edile Siracusana, Siracusa, pp 89–115
Lipscombe PR, Pellegrino S (1993) Free rocking of prismatic blocks. J Eng Mech 119:1387–1410. doi:10.1061/(ASCE)0733-9399(1993)1197(1387)
Peña F, Prieto F, Lourenço PB, Campos-Costa A, Lemos JV (2007) On the dynamics of rocking motion of single rigid-block structures. Earthq Eng Struct Dyn 36:2383–2399. doi:10.1002/eqe.739
Plaut RH, Fielder WT, Virgin LN (1996) Fractal behavior of an asymmetric rigid block overturning due to harmonic motion of a tilted foundation. Chaos Soliton Fract 7:177–196
Priestley MJN, Evison RJ, Carr AJ (1978) Seismic response of structures free to rock on their foundations. Bull New Zealand Natl Soc Earthq Eng 11:141–150
Rankine WJM (1863) A manual of civil engineering, 2nd edn. Griffin Bohn, London
Shenton HWIII (1996) Criteria for initiation of slide, rock, and slide-rock rigid-body modes. J Eng Mech 122:690–693. doi:10.1061/(ASCE)0733-9399(1996)122:7(690)
Sorrentino L, Masiani R, Decanini LD (2006a) Overturning of rocking rigid bodies under transient ground motions. Struct Eng Mech 22:293–310
Sorrentino L, Mollaioli F, Masiani R (2006b) Overturning maps of a rocking rigid body under scaled strong ground motions. 1 European conference on earthquake engineering and seismology, Geneva, 3–8 September 2006
Sorrentino L, Kunnath S, Monti G, Scalora G (2008a) Seismically induced one-sided rocking response of unreinforced masonry façades. Eng Struct 30:2140–2153. doi:10.1016/j.engstruct.2007.02.021

Sorrentino L, Masiani R, Griffith MC (2008b) The vertical spanning strip wall as a coupled rocking rigid body assembly. Struct Eng Mech 29:433–453

Sorrentino L, Masiani R, Benedetti S (2008c) Experimental estimation of energy damping during free rocking of unreinforced masonry walls. First Results. 2008 Seismic engineering international conference commemorating the 1908 Messina and Reggio Calabria earthquake, Reggio Calabria, 8–11 July 2008

Spanos PD, Roussis PC, Politis NPA (2001) Dynamic analysis of stacked rigid blocks. Soil Dyn Earthq Eng 21: 559–578. doi:10.1016/S0267-7261(01)00038-0

Tobriner S, Comerio M, Green M (1997) Reconnaissance report on the Umbria-Marche Italy earthquake of 1997. EERI Newsl 31

Yim CS, Chopra AK, Penzien J (1980) Rocking response of rigid blocks to earthquakes. Earthq Eng Struct Dyn 8:565–587